

# Quantitative Evaluation of Solidification Brittleness of Weld Metal during Solidification by Means of In-Situ Observation and Measurement (Report I

— Development of the MISO Technique —

Fukuhisa MATSUDA\*, Hiroji NAKAGAWA\*\*, Kazuhiro NAKATA\*\*\*, Hiroaki KOHMOTO\*\*\*\* and Yoshiaki HONDA\*\*\*\*\*

## Abstract

A new technique named MISO technique to evaluate brittleness or ductility of solidifying weld metal has been invented, and its applicability has been studied in tensile hot cracking test for plain carbon steels, austenitic stainless steels and aluminum alloys, in which weld metal during solidification is photographed with microscope and high speed cinecamera, and the marks in the photographs due to ruggedness or structure on the weld metal surface are utilized as the reference points of the gage length to evaluate the strain or ductility. The MISO technique has given good reproducibility of the minimum ductility required to cause cracking ( $\epsilon_{\min}$ ), if adequate range of the gage length has been adopted. The value of  $\epsilon_{\min}$  measured with the MISO technique has been fairly higher than that measured with the Trans-Varestraint test. However,  $\epsilon_{\min}$  measured with the MISO technique combined with the Trans-Varestraint test has given the similar value to that obtained with the MISO technique combined with the tensile hot cracking test. Ductility curve also has been well constructed, and thus the temperature showing  $\epsilon_{\min}$  has been easily revealed with the MISO technique.

KEY WORDS: (Solidification) (Hot Cracking) (Carbon Steels) (Photography) (Welding)

## 1. Introduction

Hot cracking, especially solidification cracking, is one of the serious problem affecting weldability, and thus many cracking tests have been invented or developed. Although they have been used properly according to their applicability for the purpose of comparison of crack susceptibilities, most of them can't give any information about the ductility of solidifying weld metal quantitatively. Among them, it is well known that the Trans-Varestraint test<sup>1)</sup> which was developed from original RPI Varestraint test<sup>2)</sup> by one of the authors can evaluate the ductility of weld metal by very simple procedure, and thus ductility curve which gives the relation between temperature and ductility can be constructed easily. On the basis of ductility curve, many valuable parameters such as brittleness temperature range (BTR), minimum ductility required to cause cracking ( $\epsilon_{\min}$ ) and critical strain rate (CST) are utilized to discuss the crack suscepti-

bility. The Trans-Varestraint test, however, is sometimes helpless in evaluation of  $\epsilon_{\min}$  when the value is too small as seen in such alloys as fully austenitic stainless steels and some aluminum alloys<sup>1), 3)</sup>.

On the other hand, hot cracking is regarded as serious in the field of continuous casting, and thus evaluation of ductility during solidification has been attempted in practical and laboratory scales by FEM<sup>4)-6)</sup>. The values of ductility obtained in continuous casting do not necessarily agree with each other, and are generally higher than those obtained with the Trans-Varestraint test. Although the difference in solidification conditions is maybe one of the reason for the disagreement, applicability of the method of measurement and analysis to evaluate the ductility in complex condition of solid-liquid coexistent region should be examined from fundamental viewpoint. In this sense, direct measurement of the strain of solid-liquid coexistent region has been eagerly waited.

† Received on April 30, 1983

\* Professor

\*\* Research Instructor

\*\*\* Research Associate

\*\*\*\* Graduate student of Osaka Univ., now with Mitsubishi Metal Corporation

\*\*\*\*\* Research Associate, Kurume Technical College

Transactions of JWRI is published by Welding Research Institute of Osaka University, Ibaraki, Osaka 567, Japan

The authors' recent paper<sup>7)</sup> has thrown light upon the direct measurement of the strain of solid-liquid coexistent region, because this paper has discussed a technique which makes it possible to analyze the crack initiation and propagation behaviors using direct observation technique of solidification front with microscope and high speed cinecamera. This suggests that evaluation of the strain or the ductility is possible if any reference points necessary for setting up gage length are photographed in high speed cinefilm. Thus the authors have thought of utilizing many marks in cinefilms, which is photographed due to the ruggedness or structure on the surface of weld metal, as the reference points. This paper discusses about the feasibility and applicability of this new technique named the MISO (masurement by means of in-situ observation) technique.

**2. Principle of the MISO Technique**

The MISO technique utilizes measurement of strain of weld metal by picture analysis method after in-situ observation of weld metal during solidification with optical microscope and high speed cinecamera (or high speed video technique). For example, Fig. 1 shows a sequence of high speed photographs which was taken during tensile

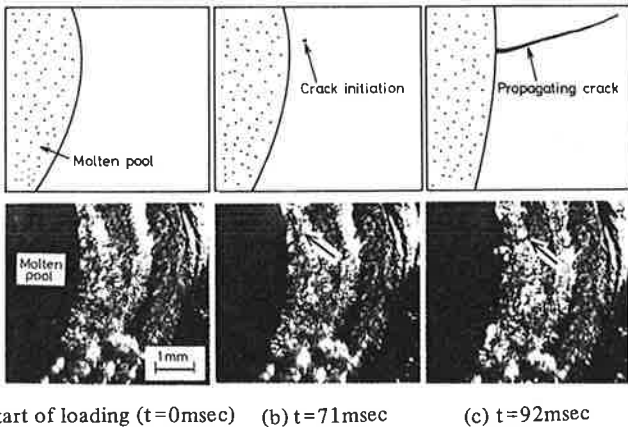


Fig. 1 An example of sequence of high speed photographs during tensile hot cracking test of plain carbon steel

hot cracking test of plain carbon steel, of which the procedure is discussed later. Figure 1(a), (b) and (c) shows the start of loading, the moment of the initiation of a crack and propagating crack, respectively. It should be noticed that there are many spotty marks owing to ruggedness or structure of the surface of weld metal. Thus the authors had the conception that these marks can be utilized as the reference points of gage length to measure the strain or the ductility of solidifying weld metal.

As well known, the characteristic of ductility can be fully expressed by "ductility curve"<sup>1)</sup> which gives the relation between temperature and ductility. In the case of rapid tensile hot cracking test discussed in this paper the authors used two types of method, namely "Fixed Gage Method" and "Moving Gage Method" to complete the ductility curve.

The procedure of the Fixed Gage Method is illustrated in Fig. 2, where the loading direction is perpendicular to the welding direction. At the first place, as the reference

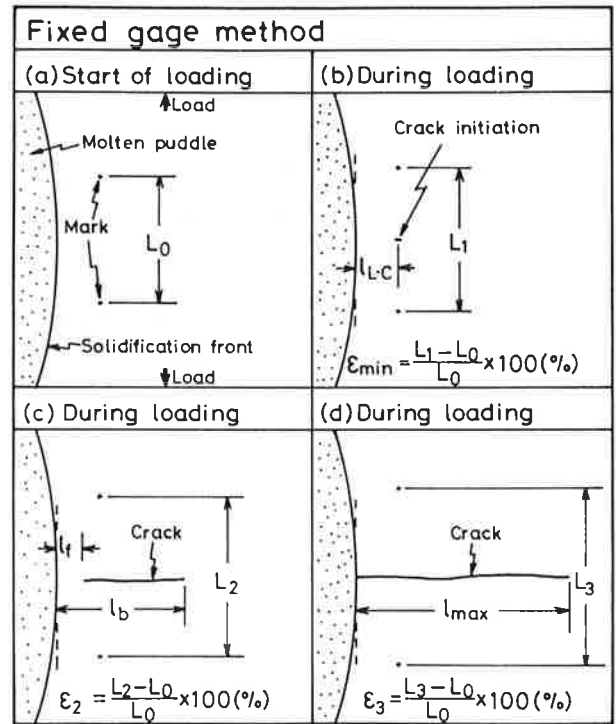


Fig. 2 Illustration of procedure of Fixed Gage Method

points of gage length, two marks facing each other across the crack initiation site are chosen as seen in Fig. 2(a). In practice these two marks can be selected by rewinding the cinefilm, watching the cine photographs projected on the screen of a film motion analyzer. Of course the direction of the line connecting these two marks must be parallel to the loading direction. Suppose that crack initiation occurs when the gage length which is  $L_0$  at the instant of the start of loading increases to  $L_1$  as seen in Fig. 2 (b). Now, the minimum ductility required to cause cracking,  $\epsilon_{min}$ , can be calculated by the equation written in Fig. 2(b), and the location of crack initiation from the solidification front  $l_{L-C}$  is recorded. The crack in Fig. 2(c) propagates up to  $l_f$  and  $l_b$  when the gage length is  $L_2$  and thus the strain is  $\epsilon_2$  as written in Fig. 2(c). Finally the crack in Fig. 2(d) reaches the saturated location  $l_{max}$  when the gage length is  $L_3$  and the strain is  $\epsilon_3$ . In the

calculation of  $\epsilon_2$  and  $\epsilon_3$ , the width of the crack is subtracted from the gage length. The distances  $l_{L-C}$ ,  $l_f$ ,  $l_b$  and  $l_{max}$  can be easily converted into their temperature differences and temperature range by measuring the temperature distribution of weld metal with thermocouple.

The procedure of the Moving Gage Method is illustrated in Fig. 3, where several couples of two marks as the reference points are chosen. Each couple is used for the

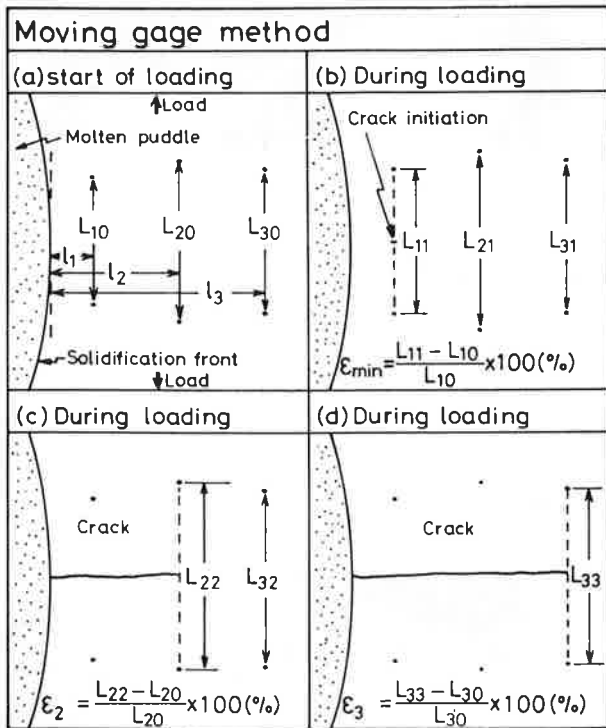


Fig. 3 Illustration of procedure of Moving Gage Method

evaluation of the strain at only its location as seen in Fig. 3. In other words, the reference points are always reset to the place across the growing crack tip. In principle the Moving Gage Method gives the ductility curve more precisely than the Fixed Gage Method, but the procedure is relatively troublesome.

In both methods, initial gage length  $L_0$  is very important in relation to the accuracy of the ductility measured. Since spontaneous marks are used as the reference points in the MISO technique, constant initial gage length cannot be chosen essentially, and thus optimum range of the initial gage length must be determined before the testing. This is discussed later.

### 3. Application of the MISO technique to Tensile Hot Cracking Test

#### 3.1 Materials used and testing procedure

Tentative plain carbon steels, commercial austenitic stainless steels and commercial aluminum alloys were used, and their chemical compositions are shown in Table 1. The general configuration of the specimen is shown in Fig. 4, which has two holes for pins of chuck and notches to concentrate deformation to weld metal which is illustrated by broken line.

The specimen together with a microscope, a high speed cinecamera and a TIG torch was set to a horizontal tensile cracking tester, which has the maximum crosshead speed of about 10 mm/sec, as shown in Fig. 5. The microscope has a large working distance of 87 mm and zooming mechanism from x0.66 to x4 in objective lens so that optimum magnification depending on the kind of material

Table 1 Chemical composition and thickness of materials used

(a) Steels									
Material	Item	Composition (wt.%)							Thickness (mm)
		C	Si	Mn	P	S	Cr	Ni	
Plain carbon steel	08C	0.08	0.14	0.28	0.010	0.003	-	-	4
	08C-S	0.08	0.14	0.29	0.010	0.021	-	-	4
	16C	0.16	0.14	0.28	0.010	0.004	-	-	4
	30C	0.31	0.14	0.28	0.010	0.004	-	-	4
	30C-P	0.29	0.15	0.29	0.020	0.005	-	-	4
	50C	0.50	0.14	0.29	0.010	0.005	-	-	4
Austenitic stainless steel	SUS304L*	0.02	0.59	0.99	0.028	0.013	19.09	9.75	2
	SUS310S*	0.07	0.80	1.55	0.016	0.005	25.00	20.08	2

(b) Aluminum alloy										
Item	Composition (wt.%)									Thickness (mm)
	Si	Fe	Cu	Mn	Mg	Cr	Zn	Ti	B	
A5052*	0.09	0.23	0.01	0.04	2.25	0.20	0.02	0.01	-	2
A5083*	0.11	0.21	0.01	0.56	4.73	0.09	0.02	0.02	0.0007	2

\* Designation follows Japan Industrial Standard (JIS)

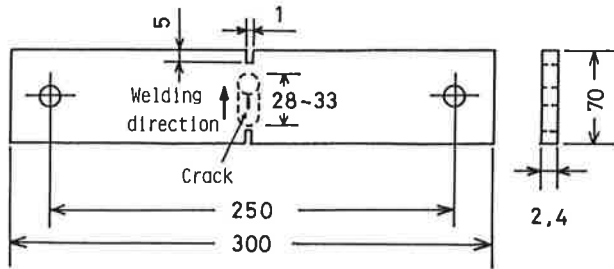


Fig. 4 General configuration of cracking test specimen

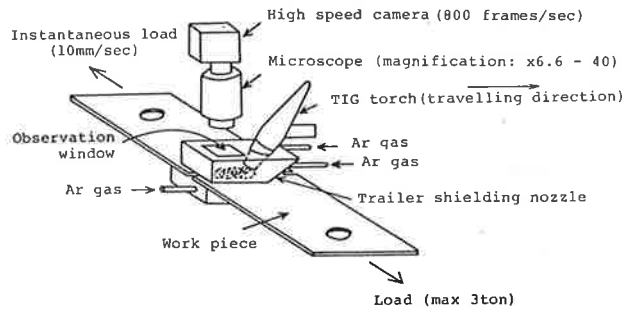


Fig. 5 Illustration of arrangement of equipments in the MISO technique combined with tensile hot cracking test

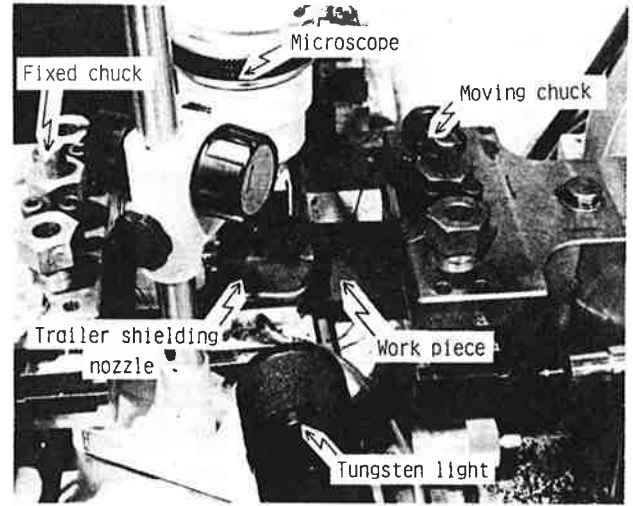


Fig. 6 Close-up view of the arrangement in the MISO technique combined with tensile hot cracking test

Table 2 Welding conditions and image magnification in cinefilm

Material	Welding conditions			Image magnification in cinefilm
	Welding current (A)	Arc voltage (V)	Welding speed (mm/min)	
Plain carbon steel	90	19.5	10	1.9
Austenitic stainless steel	65	18.5	10	1.3
A5052	50 (DCRP)	21	100	1.3
A5083	50 (DCRP)	21	100	1.9

and welding condition may be chosen. The TIG torch has a specially designed trailer shielding nozzle with a glass window on the top through which in-situ observation was done. Moreover a vertical illumination system with a tungsten light and a half-mirror was utilized to improve image contrast, though they are omitted in Fig. 5. Close-up view of the testing assembly is shown in Fig. 6.

When the TIG torch passed near the middle of whole weld length, the specimen was pulled perpendicularly to the weld line in the maximum crosshead speed. In this crosshead speed the mean strain rate near the center of the weld metal just behind the solidification front was about 130%/sec. Just before the pulling, the high speed cine-camera was started at about 800 frames/sec. The welding conditions and the image magnification in the cinefilm are given in Table 2. An example of the bead surface after the cracking test is shown in Fig. 7, where several cracks are formed behind the crater corresponding to the solidification front at the moment of pulling. The temperature distribution in the weld metal was measured with W/5%Re-W/26%Re thermocouple of 0.3 mm diam.

The cinefilm after development was set to a film motion analyzer by which the photographs projected on its screen in a magnification of 20 times the image magnification in cinefilm was analyzed with its cursors on the screen to measure the strain by the procedure discussed in Figs. 3 and 4.

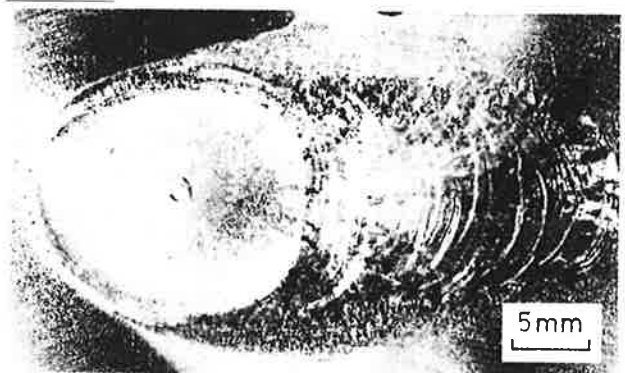


Fig. 7 Appearance of surface of weld metal after cracking test

### 3.2 Determination of optimum gage length

Figure 8(a) and (b) show the dependence of the minimum ductility  $\epsilon_{min}$  on the gage length  $L_0$  in plain carbon steels and SUS304L, respectively. The value of  $\epsilon_{min}$  gradually increases together with the decrease in  $L_0$ , and its scatter is large in the range of  $L_0$  less than about 0.9 mm. As already mentioned, constant gage length cannot be chosen in the MISO technique, because spontaneous marks are used as the reference points. Thus,  $L_0$  between 0.9 and 1.7 was determined to be utilized. The

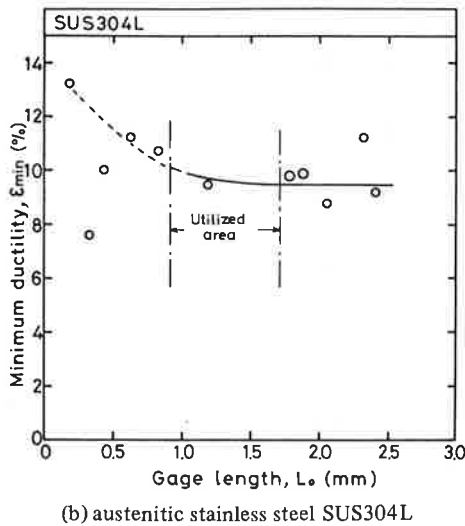
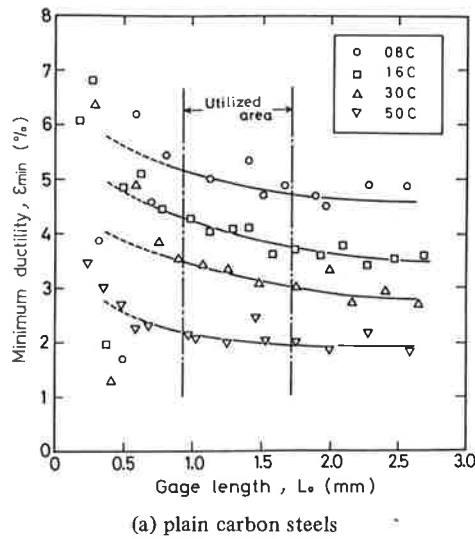


Fig. 8 Variation of minimum ductility  $\epsilon_{min}$  with gage length  $L_0$

relative scatter in this range was within about 10% of  $\epsilon_{min}$ .

In order to reveal the reason why the scatter of  $\epsilon_{min}$  is large in the small value of  $L_0$ , the strain distribution perpendicular to the weld axis was studied using small  $L_0$  between 0.32 and 0.47 for SUS304L. The result is shown in Fig. 9, in which coordinates  $x$  and  $y$  are defined in Fig. 10, and the location of  $x$  in Fig. 9 is fixed to 0.13 mm. Now crack initiation occurred at a location of  $x=0.13$  mm and  $y=0$  mm. Figure 9 means that strain concentration gradually developed at  $y=-0.7, 0$  and  $0.9$  mm with the lapse of time after the start of loading, and that finally the strain at  $y=0$  mm reached the intrinsic  $\epsilon_{min}$  fastest. Analysis of the microstructure of the weld metal revealed that strain concentration occurred at grain boundaries of columnar crystals. Therefore it is understood that the scatter of  $\epsilon_{min}$  in the small range of  $L_0$  in Fig. 8 occurred

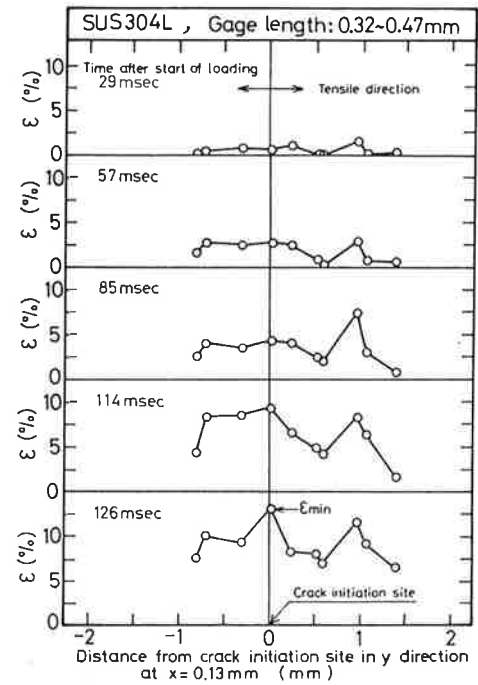


Fig. 9 Strain distribution near crack initiation site perpendicular to weld axis during cracking test of SUS304L

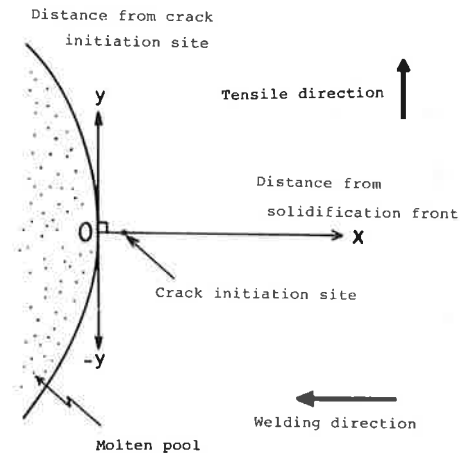


Fig. 10 Definition of coordinates  $x$  and  $y$

due to the nonuniform strain distribution caused by strain concentration at grain boundaries.

### 3.3 Examples of ductility curves

Figure 11(a), (b) and (c) show the ductility curves by the Fixed Gage and the Moving Gage Methods for plain carbon steel 08C-S, fully austenitic stainless steel SUS310S and aluminum alloy A5052. The limit of ductility curve in its higher temperature side is set to the liquidus temperature which was measured by thermal analysis in an electric furnace. Next three phenomena are noteworthy

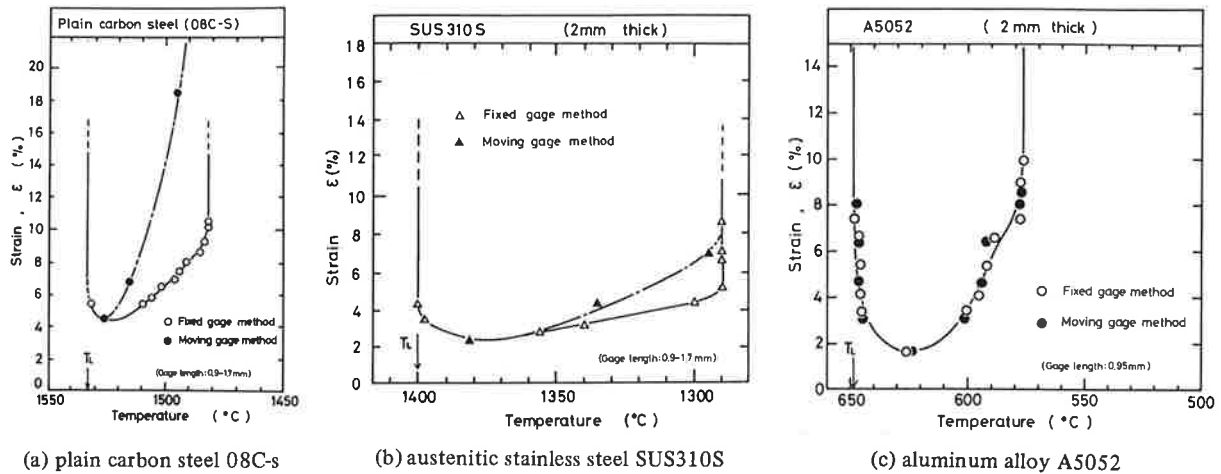


Fig. 11 Comparison of ductility curves between Fixed Gage and Moving Gage Methods

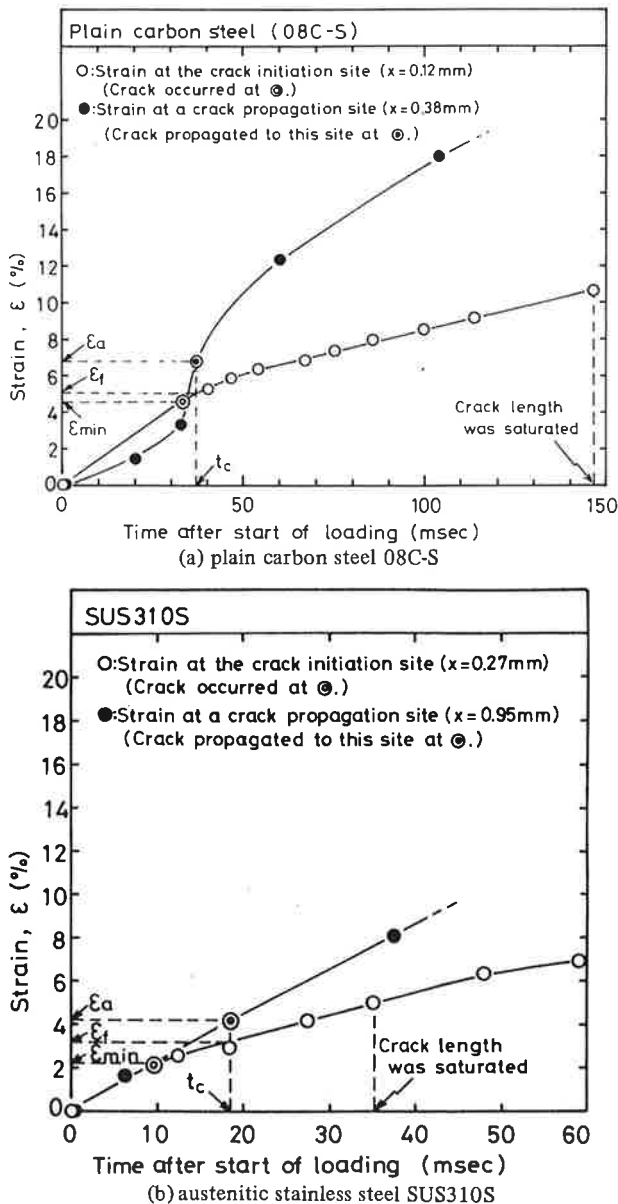


Fig. 12 Comparison of strain accumulations between the crack initiation site and a crack propagation site

in Fig. 11: (i) The ductility curves by the Fixed Gage and the Moving Gage Methods nearly agree with each other except for 08C-S. (ii) The minimum ductilities are fairly higher than those measured with the Trans-Varestraint test<sup>1), 3), 8)</sup>. (iii) The temperature showing  $\epsilon_{min}$  is clearly recognized.

As regards the phenomenon (i), the developments of the strain at the crack initiation site and a crack propagation site were compared with each other for 08C-S and SUS310S, where the strains were measured with the reference points fixed to these sites, respectively. The results are shown in Fig. 12(a) and (b), in which  $x$  has the same definition as in Fig. 10. In Fig. 12 (a) the values of  $x$  at the crack initiation and the propagation sites are 0.12 and 0.38 mm respectively, and thus the distance between them is 0.26 mm. When  $t$  was  $t_c$  ( $=38$  msec), the crack reached the propagation site, and it should be noticed that sudden increase in the strain at the propagation site occurred just before  $t_c$ , though such increase didn't occur at the initiation site just before  $t_c$ . This means that there was much strain concentration at the growing crack tip due to the high resistance to solidification crack. Therefore the ductility of the crack propagation site evaluated by the Fixed Gage Method, which corresponds to  $\epsilon_f$  in Fig. 12(a), was distinctly less than the ductility evaluated by the Moving Gage Method, namely  $\epsilon_a$ . In Fig. 12(b) the values of  $x$  at the crack initiation and the propagation sites are 0.27 and 0.95 mm, and thus the distance between them is 0.68 mm. When  $t$  was  $t_c$  ( $=18$  msec), the crack reached the propagation site, but sudden increase in the strain didn't occur even at the propagation site. Moreover the difference between  $\epsilon_f$  and  $\epsilon_a$  was not so much in spite of the longer distance between the initiation and propagation sites than in Fig. 12(a). This means that there was only a little strain concentration at the growing crack tip.

In principle the Moving Gage Method should be recommended, but is relatively troublesome in measuring procedure. Moreover the value of  $\epsilon_{\min}$ , which is considered to be the most important parameter in the MISO technique<sup>9)</sup>, is completely the same in both methods. Furthermore precise ductility curve may be necessary for materials susceptible to crack, in which the both methods give nearly the same ductility curves. Considering these, it may be concluded that even the Fixed Gage Method is satisfactory in most case. For some aluminum alloys

susceptible to crack, however, the Moving Gage method should be compelled to be used<sup>10)</sup>, because the image magnification in cinefilms enough to photograph the long crack into one frame of the film is too low to evaluate the strain precisely, and thus because photographing in twice which is aimed at the high and low temperature regions of the long crack is necessary.

As regards the phenomenon (ii), Table 3 summarizes the values of  $\epsilon_{\min}$  measured with the MISO technique and

Table 3 Comparison of  $\epsilon_{\min}$  between the MISO technique and the Trans-Varestraint test

Material	Item	$\epsilon_{\min}$ (%)					
		MISO technique		Ordinary Trans-Varestraint test			
		Tensile test	Trans-Varestraint test	This study	Ref. 1	Ref. 3	Ref. 8
Plain carbon steel	08C	4.9	-	-	-	-	-
	08C-S	4.3	-	-	-	-	-
	SW*(0.12%C)	-	-	-	0.5-0.75	-	-
	16C	4.3	-	-	-	-	-
	SS41**(0.22%C)	-	-	-	<0.15	-	-
	30C	3.4	-	-	-	-	-
	30C-P	2.0	1.7	<0.5	-	-	-
Austenitic stainless steel	50C	2.1	-	-	-	-	-
	S55C**(0.55%C)	-	-	-	<0.15	-	-
	SUS304(L)**	9.0	-	-	0.5-0.75	-	0.6
Aluminum alloy	SUS310S**	2.3	-	-	<0.15	-	0.08
	A5052**	1.6	-	-	-	<0.1	-
	A5083**	2.1	-	-	<0.15	<0.1	-

\* Submerged arc weld metal

\*\* Designation follows Japan Industrial standard (JIS)

with the Trans-Varestraint test<sup>1),3),8)</sup>. It is clearly seen that the values of  $\epsilon_{\min}$  measured with the MISO technique are fairly higher than those with the Trans-Varestraint test. In order to reveal the reason for this difference,  $\epsilon_{\min}$  of a plain carbon steel 30C-P was also measured with the MISO technique combined with the Trans-Varestraint test. This result is also shown in Table 3, and it is understood that the MISO technique combined with the Trans-Varestraint test gives nearly the same  $\epsilon_{\min}$  value as that measured with the MISO technique combined with the tensile hot cracking test. This suggests that the low value of  $\epsilon_{\min}$  in the ordinary Trans-Varestraint test may be caused by disregard for the local strain concentration near the solidification front in excess of nominal strain evaluated by the thickness of specimen and the radius of bending block<sup>1)</sup>.

Now, Fig. 13 shows the progress of the strain distribution in x direction after the start of loading for SUS304L. It is seen that strain gradually concentrated near the solidification front with the lapse of time after the start of loading. The reason for this strain concentration near the solidification front is considered to be temperature distribution affecting deformation characteristics and existence of molten puddle acting as strain concentrator.

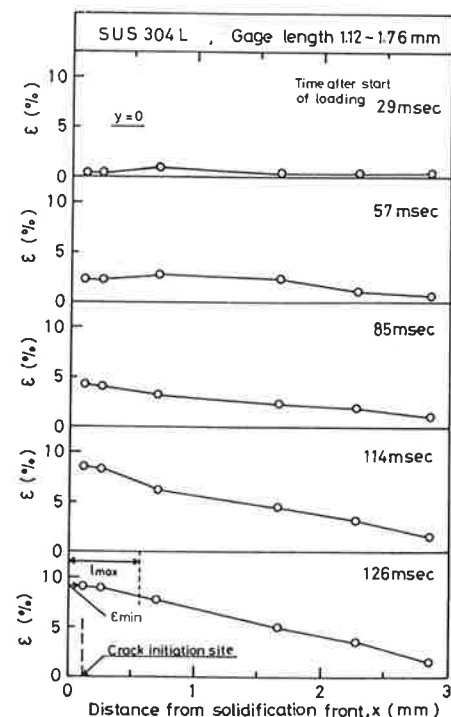


Fig. 13 Strain distribution near solidification front along weld axis during cracking test of SUS304L

Therefore it may be concluded that the MISO technique gives more reasonable or accurate  $\epsilon_{\min}$ . Of course, as seen in Fig. 8, even  $\epsilon_{\min}$  measured with the MISO technique does not give the true value because of the dependence of  $\epsilon_{\min}$  on the gage length.

As regards the phenomenon (ii), the crack initiation temperature generally locates in high temperature region in BTR<sup>7), 9)</sup>, and this behavior is generally related to the distribution of remaining interdendritic liquids<sup>7)</sup>.

#### 4. Conclusions

The principle and the procedures of the newly developed MISO technique to evaluate the brittleness of solidifying weld metal have been studied and discussed. Main conclusions obtained are as follows:

- 1) In the MISO technique, weld metal during solidification is photographed with microscope and high speed cinecamera, and the marks in the photographs due to ruggedness or structure on the weld metal surface are utilized as the reference points of the gage length to evaluate the strain and ductility.
- 2) The MISO technique, which has been mostly combined with tensile hot cracking test in this paper, gives good reproducibility of the minimum ductility required to cause cracking ( $\epsilon_{\min}$ ), if adequate range of gage length is adopted. The range of the adequate gage length used in this paper was 0.9 to 1.7 mm for steels.
- 3) The value of  $\epsilon_{\min}$  measured with the MISO technique is fairly higher than that measured with the Trans-Varestraint test. However,  $\epsilon_{\min}$  measured with the MISO technique combined with the Trans-Varestraint test gives the similar value to that measured with the MISO technique combined with the tensile hot cracking test.
- 4) In the MISO technique Fixed Gage and Moving Gage Methods are available to construct the ductility curve which gives the relation between temperature and ductility. In the Fixed Gage Method the reference points to measure the change in gage length are fixed at the crack initiation site. In the Moving Gage Method, the reference points are reset to the growing crack tip. Although the Moving Gage Method should give more accurate ductility curve in principle, the ductility curves obtained with both methods nearly coincide with each other except for the material insusceptible to solidification crack.
- 5) Another excellent characteristic of the MISO technique is that it clearly reveals the temperature showing  $\epsilon_{\min}$ , namely crack initiation temperature.

#### Acknowledgement

The authors would like to thank Mr. Y. Takeuchi, formerly student of Kinki Univ., for his cooperation in the experiment, and Committee on Mechanics Behavior of Solidification in Continuous Casting (Chairman Prof. T. Mori) of the Japan Iron and Steel Institute for its supply of materials.

#### References

- 1) T. Senda, et al: Trans. Japan Weld. Soc., Vol. 2 (1971), No. 2, p. 1.
- 2) W.F. Savage and C.D. Lundin: Weld. J., Vol. 44 (1965), 433s.
- 3) Y. Arata, et al: Trans. JWRI, Vol. 5 (1976), No. 2, p. 153.
- 4) K. Narita, et al: J. Iron & Steel Inst. Japan, Vol. 66 (1980), s806 (in Japanese).
- 5) K. Narita, et al: J. Iron & Steel Inst. Japan, Vol. 67 (1981), p. 1307 (in Japanese).
- 6) T. Matsumiya, et al: J. Iron & Steel Inst. Japan, Vol. 69 (1983), s169 (in Japanese).
- 7) F. Matsuda, et al: Trans. JWRI, Vol. 11 (1982), No. 2, p. 67.
- 8) Y. Arata, et al: Trans. JWRI, Vol. 6 (1977), No. 1, p. 105.
- 9) F. Matsuda, et al: Trans. JWRI, Vol. 12 (1983), No. 1, p. 73.
- 10) F. Matsuda, et al: Unpublished.